

On the use of AESA (Active Electronically Scanned Array) Radar andIRST (InfraRed Search&Track) System to Detect and Track Low Observable Threats

George-Konstantinos Gaitanakis¹, George Limnaios², and Konstantinos C. Zikidis^{2,✉}

¹Hellenic Army Academy, Vari, Attika, Greece

²Hellenic Air Force Academy, Dekelia Air Base, Attika, Greece

Abstract. The radar has been indisputably the most important sensor in the battlefield, allowing early warning and tracking of air vehicles. Modern fighter aircraft employing AESA fire control radars are able to acquire and track targets at long ranges, in the order of 50 nautical miles or more. However, the proliferation of low observable or stealth technology has contested radar capabilities, reducing their detection / tracking ranges roughly to one third. This degradation is more severe concerning fighter aircraft radars, since most stealth threats are optimised for higher frequency bands, as in the case of fire control radars. Hence, other parts of the electromagnetic spectrum have been reconsidered, such as infrared radiation (IR). Every aircraft is a source of IR, due to fuel combustion, aerodynamic friction and IR reflection. In this way, a jet fighter can be detected by an IR sensor against the cold background of the sky. Therefore, IRST systems have re-emerged, offering an alternative to the radar. Apart from their capabilities concerning target detection (whether stealth or not), IRST systems also exhibit passive operation, resilience to jamming and better angular accuracy. On the other hand, they are prone to weather conditions, especially moisture, while they cannot measure distance directly, as in the case of the radar. This work explores and compares the capabilities and limitations of the two approaches, AESA radars and IRST systems, offering also some insight to the benefits of sensor fusion.

1 Introduction

Most jet fighters today are equipped with mechanically scanned antenna (MSA) radars, where the beam is steered by mechanically deflecting a planar antenna. Despite the maturity and the decent performance of such radar systems, the conventional gimballed antenna is limited by inertia. Thus, the electronically scanned array (ESA) has been introduced, consisting of a large number of radiating elements, where the beam can be steered by controlling the phase shift individually for each element [1]. Agile beam steering

✉ Corresponding author: kzikidis@cs.ntua.gr

via electronic control of beam direction is the main advantage of ESA over MSA, as it permits flexible control of the beam for tracking individual targets or groups of targets [2].

These antennae are often known as phased arrays and they fall into two categories, passive and active ESA (PESA and AESA), depending on where the power is produced: PESA systems employ a conventional transmitter, based usually on one or two Travelling Wave Tubes (TWT), providing the necessary RF power, and a computer-controlled phase shifter just before every radiating element, while AESA systems consist of Transmit-Receive Modules (T/R modules or TRM), which combine independently controlled transmitters, receivers, and beamsteering controls, usually by phase [2][3].

AESA systems offer significant benefits in terms of beam agility, operational exploitation diversity and reliability. TRMs are based mainly on Gallium Arsenide (GaAs) technology. However, due to the poor thermal conductivity of GaAs, more recently silicon germanium (SiGe) and especially Gallium nitride (GaN) are emerging, with the latter being considered for all advanced AESA development programs [1][4].

Radar systems are challenged by low observable techniques, aiming at the reduction of the RCS (Radar Cross Section). In this way, electro-optical sensors andIRST systems in particular offer significant advantages.

However, all available sensors should be taken into account in order to "build" spherical situational awareness. Therefore, multi sensor data fusion is required, for target tracking based on measurements from different sources, avoiding multiple tracks. Every sensor exhibits certain advantages and limitations, while their synergy provides an operationally useful conjunction.

In the next section, issues concerning the AESA technology will be discussed, analysing the case of MSA to AESA upgrade and the relevant limitations thereof. Consequently, theIRST potentials will be examined, providing a comparison between radar andIRST against stealth aircraft. Finally, the benefits of the multi sensor data fusion will be discussed.

2 On the use of AESA Radars

A fighter aircraft AESA radar is composed of 1000-2000 TRMs, each comprising a high power amplifier (HPA), a radiating element (typically a dipole or a waveguide slot), a low noise amplifier (LNA), a variable-gain amplifier and variable phase shifter, and a digital control circuit. Each TRM is individually controlled, generating its own signal, allowing for advanced possibilities such as numerous simultaneous "sub-beams" in different frequencies.

2.1 AESA drawbacks - limitations

The AESA advantages have been properly documented in the literature (and well advertised). On the other hand, AESA radars are stated to cost roughly 50% more than their MSA equivalent, while they suffer from certain issues, discussed in the following sections.

2.1.1 Scan loss due to off-boresight angle

As the angle θ between the broadside of the antenna (the boresight line) and the beam increases, the antenna gain, the beamwidth and subsequently the directivity and angular resolution deteriorate, as a function of $\cos(\theta)$. This is an inherent characteristic of phased arrays, due to geometry, practically limiting their use up to an off-boresight angle of 60° .

Concerning the gain, the one-way scanning loss would be expected to be proportional to $\cos\theta$, since this is the reduction in projected area [6]. However, in practice, this is the minimum loss, due to active impedance (or mutual coupling) mismatch at the radiating

element level. This additional gain loss contribution is of the order of $\cos^{0.3} \theta$ to $\cos^{0.5} \theta$, depending on the particular antenna, so the total roll-off is $\cos^{1.3} \theta$ to $\cos^{1.5} \theta$. In general, scan loss is in the form of some power of the cosine $\cos^n \theta$, with $n \approx 1.5$ commonly used [7]. Obviously, this has an impact on maximum detection range as well. This issue is well known, e.g., in 2009 it was reported that "the fixed array loses performance at high off-boresight angles, and at angles above 45° it is less effective than a MSA" [8].

2.1.2 Power and cooling requirements

All currently operational fighter AESA radars are based on GaAs technology. As mentioned before, such modules exhibit poor thermal performance. Heat must be conducted out of the array by liquid cooling, typically with Coolanol or PAO coolant.

Concerning the power efficiency of a T/R module, the most common metric is the Power Added Efficiency (PAE), which refers to the efficiency of the final stage, i.e., of the High Power Amplifier (HPA). Currently GaAs HPAs can exceed 40% PAE at the X-band, while GaN amplifiers can offer more than 50%. On the other hand, TWTs may deliver more than 60% efficiency. However, there are other elements consuming power on each T/R module, such as switching circuitry, the LNA, and the module control circuit [1]. The power consumed by all other elements except for the HPA is the overhead power. It is evident that the overall module efficiency is considerably lower than the PAE.

In [9], there is a diagram of the overall TRM efficiency versus the HPA efficiency (PAE), for "present" (i.e., 1998) and "future" module technology. According to that graph, if GaAs TRMs are considered with a PAE of 35%, at a duty cycle of 10%, the overall T/R module efficiency would be estimated at 20% (considering "future TRM"). This means that for every kW of transmitted power, 4 kW of heat should be dissipated, not including the heat produced by the other radar parts, e.g., exciter, receiver, processor etc.

2.2 The radar equation for AESA radars

Radar range is a highly stochastic variable, depending on many parameters, including the RCS of the target, as well as its position and attitude. In order to estimate and compare ranges among different AESA radars, one should resort to the well-known radar equation and several assumptions. Using the approach described in [10] (chapter 4), the required signal-to-noise ratio (S/N) at the output of the receiver is as follows:

$$\frac{S}{N} = \frac{P_m G_t G_r \lambda^2 \sigma T_d}{(4\pi)^3 R^4 k T_0 F L L_i} \tag{1}$$

where: P_m is the mean transmitted power, G_t and G_r are the antenna transmitting and receiving gains, λ is the wavelength, σ the target's RCS, T_d the dwell time, R the range of the target, k is Boltzmann's constant, T_0 the temperature of the receiver, F the noise figure of the receiver, L the various losses and L_i the integration loss. Solving for R and taking into account that $P_t = Np$, where N is the number of TRMs and p the mean power of each TRM, as well as that $G_t = G_r = \pi N$ (on the broadside direction), this equation becomes:

$$R = \sqrt[4]{\frac{N^3 p \pi^2 \lambda^2 \sigma T_d}{(4\pi)^3 S/N k T_0 F L L_i}} \tag{2}$$

Concerning modern radars with electronic detection, the *effective detectability factor* $D_x(n')$ can be used, instead of the required S/N [11]. This term takes into account the

integration of n pulses, the type of target's RCS fluctuation (denoted by the subscript x), the probability of detection, the false alarm rate and various losses. Following section 1.4 of [11] and eq. 1.22 thereof, without the path propagation factor, the radar equation becomes:

$$R = \sqrt[4]{\frac{N^3 p \pi^2 \lambda^2 \sigma T_d}{(4\pi)^3 k T_s D_x(n) L_t L_a}} \quad (3)$$

where T_s is the total system temperature, L_t is the transmission line loss, and L_a the atmospheric absorption loss for the two-way path.

2.3 Case study for the F-16: upgrading the MSA radar with an AESA radar

Currently, the latest MSA radar on the F-16 is the Northrop Grumman AN/APG-68(V)9. According to open sources, the radar range against a standard target of 1 m² RCS is assumed to be approximately 38 nautical miles (n.m.). The required input power is 5.6 kVA, as was stated in relevant brochures, as well as other sources [12]. The aircraft provides cooling to the radar by air flow, which has been reported to be relatively marginal with respect to the requirements of this radar [12]. The cooling capacity of the aircraft for the radar is expected to be less than 5.6 kW. For the sake of discussion, one can assume 5.5 kW.

Following the APG-77 (F-22), the APG-80 (F-16E/F Block 60), as well as the APG-81 (F-35), Northrop Grumman developed the Scalable Agile Beam Radar or SABR in the mid-2000s, as a possible upgrade option for the existing F-16 fleet, designed to be installed without making any major modifications to the aircraft. Later, it was designated as AN/APG-83. According to the manufacturer, it integrates within the F-16's current structural, power and cooling constraints without Group A aircraft modification.

It can be assumed that the APG-83 has the same number of TRMs as the APG-80, i.e., 1020 TRMs. Considering GaAs TRMs of 10W each, the peak power is of the 10 kW class. Liquid cooling is used inside the radar, in order to remove the waste heat from the antenna array and the other radar parts, transferring the heat to the aircraft's air cooling system.

Apart from the antenna array, the radar comprises other LRUs (Line Replaceable Units), such as the Receiver Exciter Processor (REP) and the radar rack assembly, including the elements of the internal cooling system. Assuming that these two LRUs produce roughly 1 kW and 0.5 kW of heat, respectively, the upper limit on the antenna array waste heat is approximately 4 kW, in order not to exceed 5.5 kW in total.

Considering the available GaAs TRM technology available at the time the SABR was being developed, it can be assumed that the PAE is in the order of 35% and the overall T/R module efficiency is estimated at 20%. Therefore, the average transmitted power can be up to 1 kW, in order not to exceed 4 kW of waste heat, and the duty cycle cannot exceed 10%. This limitation has dire consequences on the detection range, since the average transmitted power is a crucial factor. In this way, the F-16E/F Block 60 was designed taking into account the cooling requirements of the APG-80, providing liquid cooling to the radar and allowing for better performance. Actually, most aircraft featuring an AESA radar provide liquid cooling.

2.4 Estimating the AESA detection range

Concerning the estimation of the detection ranges, especially in long-range High PRF mode, the *AESA Radar Calculator* was employed [13], a spreadsheet based on eq. (3) above. This proved to be a valuable tool, taking into account several aspects of the radar equation.

The main parameters used for the calculation of the APG-83 detection range were the following, while all other parameters were set to the default values as in [13]:

- Radar operational Frequency: 9.5 GHz
- Pulse Repetition Frequency (PRF): 100 kHz
- Pulsewidth: 1 μ s (in order to have duty cycle 10%)
- Fraction of radar time to be used for search: 100%
- Scan sector: $120^\circ \times 11^\circ$
- Aperture weighting algorithm: Taylor 40 dB
- Dwell time: 0.025 s
- Weather condition: clear air
- Probability of detection: 90%
- False alarm time: 120 s

Some minor corrections were deemed necessary in the calculation of the effective detectability factor in [13], taking into account eq.(4.58) in section 4.4.7 of [11]. Following the above reasoning, the APG-83 is expected to offer a detection range of 47 n.m. against a standard target of 1 m^2 RCS. This applies to the broadside direction, since at off-boresight angles, the gain is reduced due to scan loss, as explained in par. 2.1.1 (see Fig. 1).

Comparing the APG-83 to its predecessor, the APG-80, it is noted that no such cooling restrictions are expected on the F-16 Block 60. Therefore, keeping all parameters as above and setting only the PRF to 200 kHz, thus increasing the duty cycle to 20%, and following the same procedure as above, detection against the same target is estimated at 64 n.m.

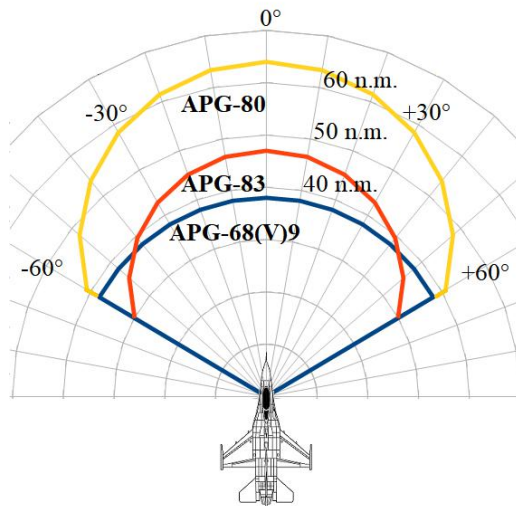


Fig. 1. Estimated detection ranges vs scan angle θ against a target of 1 m^2 RCS, for the radars APG-68(V)9, APG-83 and APG-80, assuming a scan loss of $\cos^{1.3} \theta$. At high off-boresight angles, the AESA APG-83 becomes less effective than the MSA APG-68(V)9 in terms of range.

3 On the use of IRST systems

IRST systems exhibit the following characteristics:

- a. Long detection ranges (under certain conditions), irrespectively of whether the targets are stealthy or not.
- b. Passive operation, without emitting any radiation.
- c. They cannot be easily jammed.
- d. They provide more precise angular resolution.

e. On the other hand, they are prone to weather conditions, especially moisture.

f. They cannot measure target range directly. Range measurement can be made by indirect methods.

In [5], a modern IRST was modelled and simulated against an F-35 engine model, for rear view, in various weather conditions, obtaining quite plausible results. The basic idea was, having analysed the IRST sensor, i.e., detector, optics, etc., and taking into account the weather conditions and the atmosphere transmittance, to estimate the maximum detection distance based on the radiant intensity difference between the target and the background.

Looking at an aircraft from the rear, the engine “hot parts” and the exhaust plumes emit mainly in the Medium Wave IR - MWIR window (3-5 μm). On the other hand, trying to detect an aircraft looking at it from the front involves a different mechanism: the prevalent IR source is not the engine hot parts or the exhaust plume but the skin of the aircraft, due to aerodynamic heating. However, the resultant temperatures are lower compared to rear view heat sources, thus the most suitable IR window is the Long Wave IR - LWIR (8-12 μm). If we assume 1 Mach and 218° K at 36000 ft, the stagnation temperature of the frame is: $T_t = 218^\circ \text{K} \cdot (1 + 0.164 \cdot 1^2) \approx 255^\circ \text{K}$. For the target area, a cross section of 4 m² was assumed. So, a larger target is considered (with respect to the engine nozzle) but at a much lower temperature.

Table 1. Simulation results of IRST detection range (in km), front view, at high altitude, as a function of the weather conditions, in Near/Medium/Wide Field-Of-View (FOV).

Weather Conditions	NFOV	MFOV	WFOV
Drought	44	39	35
Clean atmosphere	37	34	29
Dust - haze	22	18	15
Rainfall	17	15	13
Strong rainfall - snow	11	8	6

Following the same reasoning as in [5], the differences in the simulation are as follows:

- Pitch (distance between centres of pixels): 27 μm
- Size of each pixel or detector size: $d = 26.19 \mu\text{m}$
- Optical system diameter d_0 : $d_{near} = 138 \text{ mm}$, $d_{medium} = 69.5 \text{ mm}$, $d_{wide} = 36.66 \text{ mm}$
- Spectral detectability or specific detectivity of the detector: $D^* = 3 \cdot 10^{10} \text{ cm}\sqrt{\text{Hz}} / \text{W}$
- Wavelength: $\lambda = 12 \mu\text{m}$
- The f-number: $F\# = 0.9$
- Focal length: $f_n = 154 \text{ mm}$ (NFOV), $f_m = 62 \text{ mm}$ (MFOV), $f_w = 33 \text{ mm}$ (WFOV)
- $IFOV$ for NFOV: 0.235 mrad or 0.0125°
- Surface of the target (cross section): $A_t = 4 \text{ m}^2$
- Target (frame) temperature: $T_t = 255^\circ \text{K}$
- Bandwidth factor of the target: $n_{\Delta\lambda} = 0.38$
- Environment temperature at 36 kft: $T_b = 218^\circ \text{K}$
- Total bandwidth factor: $n'_{\Delta\lambda} = 0.10$

Taking into account the above parameters, the maximum performance of a modern IRST against a fighter at front view is depicted in Table 1.

Considering that the IRST is not dependent on the possible stealth characteristics of the target, since IRST operates in a completely different RF band, it becomes evident that such systems appear as a legitimate anti-stealth approach. On the other hand, radar systems are quite susceptible to stealth, losing rapidly their capabilities, while being vulnerable to jamming. This is depicted in Fig. 2, where the IRST is compared to the radars examined previously in Fig. 1, now against a stealth target.

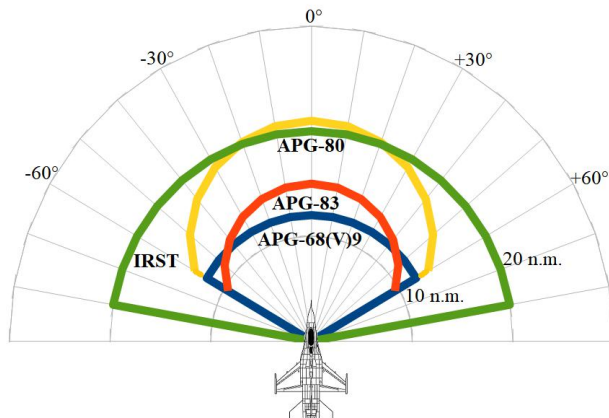


Fig. 2. Estimated maximum detection ranges vs off-boresight angle against a stealth target of 0.01 m^2 RCS (e.g., the F-35), for the APG-68(V)9, APG-83 and APG-80 radars, as well as for a modern LWIR IRST system (front view, Narrow Field Of View, clean atmosphere, at 36 kft).

4 On the use of other onboard sensors and tactical datalinks

Apart from the radar and the IRST, a fighter may employ other sensors, such as:

- the Identification Friend or Foe (IFF) system,
- other electro-optical systems, e.g., a Distributed Aperture System (DAS), a TV camera, a Forward Looking IR (FLIR), a laser rangefinder, as well as an IR missile seeker,
- the Radar Warning Receiver (RWR) of the countermeasure system, where the use of interferometry would increase considerably the localisation accuracy,
- a Laser Alert Detector,
- a Missile Approach Warning System (MAWS).

The fighter can also exchange its tactical picture in near-real time, including target tracks via a tactical datalink, such as Link 16.

Evidently, some kind of data fusion is required, in order to avoid pilot confusion: targets detected by the various sensors should be merged to one consolidated track, properly displayed. Furthermore, each sensor performs better under a different set of conditions. Therefore, the set of sensors of a combat aircraft act complementary, allowing the crew to maintain their situational awareness.

In [14] the data fusion of radar - IRST was examined, with the help of the Extended Kalman Filters. The higher angular accuracy offered by the IRST was combined with the range measurement of the radar. Simulation results showed that fusion offers better performance compared to individual sensor readings, resulting to smaller tracking error.

In this way, the datalink - IRST fusion is proposed: the information provided by the datalink (e.g., Link 16) would cue the IRST to search the target in NFOV (Narrow Field Of View), while their combination would offer a weapons quality track, without the fighter being betrayed by radar transmission. In the future, the fusion of other IRST measurements coming from friendly platforms could also be used, in a concept similar to CESMO (Cooperative Electronic Support Measures Operations).

5 Conclusion

AESA technology offers significant advantages, leading to the phaseout of traditional mechanical scanned arrays (MSAs). However, AESAs produce large amounts of heat, especially if older generation GaAs transmit/receive modules are employed. Therefore, in the case of radar upgrade from MSA to AESA, if the aircraft offers limited cooling capabilities, the mean transmitted power would have to be restricted accordingly. Taking also into account the scan loss at high off-boresight angles, the AESA upgrade would offer marginal benefit, at least in terms of range, especially against stealth aircraft.

On the other hand,IRST systems seem to be a quite promising alternative, offering adequate detection range even against stealth threats, while being discreet and immune to RF jamming.IRST could be combined with a datalink, offering weapons-quality track.

The complex modern warfare calls for data fusion of all onboard sensors and tactical datalinks, allowing the pilot to maintain spherical situational awareness, at all conditions.

References

1. G. W. Stimson, H. D. Griffiths, C. J. Baker, D. Adamy, Eds., *Stimson's Introduction to Airborne Radar, 3rd Edition*, SciTech Publishing, Edison, NJ, USA (2014)
2. C. Kopp, "Evolution of AESA Radar Technology," *Microwave Journal* (2012) <https://www.microwavejournal.com/articles/17992-evolution-of-aesa-radar-technology>
3. I. Kassotakis, "Modern Radar Techniques for Air Surveillance & Defense," *Journal of Computations & Modelling*, **4**, 1 (2014), 189-205
4. S. Piotrowicz *et al.*, "State of the Art 58W, 38% PAE X-Band AlGaIn/GaN HEMTs microstrip MMIC Amplifiers," *IEEE CSICS 2008*, 12-15 Oct., Monterey, CA (2008)
5. G.-K. Gaitanakis, A. Vlastaras, N. Vassos, G. Limnaios, and K. C. Zikidis, "InfraRed Search & Track Systems as an Anti-Stealth Approach," *Journal of Computations & Modelling*, **9**, 1 (2019), 33-53
6. M. Skolnik, *Introduction to radar systems*, 3rd Ed., McGraw-Hill Publishing Company Ltd, NY, (2001)
7. R. Mailloux, *Phased Array Antenna Handbook*, 2nd Ed., Artech House, Norwood, MA, USA (2005)
8. Bill Sweetman, "Double Vision," *Aviation Week*, Dec. (2009), pp. 43
9. R. Schaeffner, G. Eckert, and T. Nuetzel, "Design and technology of T/R modules for phased array radar applications," *Gallium Arsenide Applications Symposium GAAS 1998*, Amsterdam, The Netherlands (1998)
10. W.-D. Wirth, *Radar techniques using array antennas*, IEE, London, UK (2001)
11. D. K. Barton, *Radar equations for modern radar*, Artech House, Norwood, MA (2013)
12. D.G. Tri, *Lessons Learned From the Incorporation and Testing of the AN/APG-68 Radar on the US Naval Test Pilot School Airborne Systems Training and Research Support Aircraft (ASTARS)*, Master's Thesis, University of Tennessee (2005)
13. D. Afihandarin, *AESA Radar calculator* (2019) <https://www.mediafire.com/file/fdmzssya84htnck/AESACalcStable-ReleaseVer.xlsx/file>
14. G.-K. Gaitanakis, K. C. Zikidis and G. P. Kladis, "Multi-sensor Data Fusion for 3D Target Tracking: A Synergy of Radar and IRST (InfraRed Search & Track)," *International Scientific Conference eRA-12*, Oct. 25, 2017, Attica, Greece (2017)